

pH-Gated Photoresponsive Shuttling in a Water-Soluble Pseudorotaxane

Ander Zubillaga, Pedro Ferreira, A. Jorge Parola, Sandra Gago* and Nuno Basílio*

LAQV-REQUIMTE, Departamento de Química, Faculdade de Ciências e Tecnologia,
Universidade NOVA de Lisboa, 2829-516 Caparica, Portugal.

Email: s.gago@fct.unl.pt

Email:nuno.basilio@fct.unl.pt

Table of contents

Materials	3
Methods	3
Mathematical Model and Fitting Procedures	5
Synthesis and Characterization	7
Additional spectroscopic data	13
References	19

Materials. All solvents and chemicals employed for synthesis and for sample preparation were of reagent grade and used as received. Ultrapure Millipore grade water was used. Cucurbit[7]uril was available from previous studies.¹

Methods. The pH of the solutions was adjusted with citrate buffer, HCl and NaOH and measured with a Crison basic 20+ pH meter. UV/Vis absorption spectra were recorded with a Varian Cary 100 Bio or a Varian Cary 5000 spectrophotometer and fluorescence spectra were acquired on a SPEX Fluorolog-3 Model FL3-22 spectrofluorimeter. The titration experiments were carried out in 1 cm pathlength quartz cells. Two stock solutions are prepared for these titrations: one with only compound **1** or **2** in water at desired pH and a second one with exactly the same concentration of **1** or **2**, the same pH and known concentration of CB7 in excess. Then, a known volume of the first solution is placed in a quartz cuvette and small aliquots of the second solution are added to the cuvette and spectra registered. Using this method, the concentration of dye is kept constant during the titration while the concentration of host is increased until the no more spectral variations are observed. For the fluorescence experiments, solutions with absorbance values below 0.1 at the excitation and higher wavelengths were always used. The excitation wavelength was set at the quasi-isosbestic point ($\lambda_{\text{ex}} = 445$ nm, determined from the absorption spectra) and the emission and excitation slits were set to 1 nm.

The fluorescence quantum yields of the flavylum **2** and the respective pseudorotaxane were determined using acridine orange ($\phi=20\%$) in basic ethanol as reference.² The quantum yield of **2** (1.6 μM) in the absence and presence of 1 equivalent of CB7 was determined to be 0.9% and 17.9%. Because under these diluted conditions the fraction

of 1:1 complex ($K = 1 \times 10^7 \text{ M}^{-1}$) is 0.73 and assuming that the observed quantum yield is given by mole fraction averaged quantum yields of the free (ϕ_f) and complexed species (ϕ_c) (equation S1), the quantum yield of the 1:1 pseudorotaxane was calculated to be 24%.

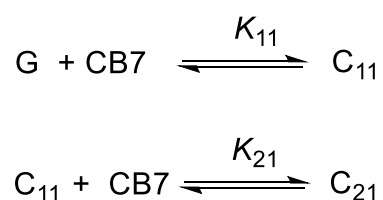
$$\phi_{obs} = \chi_f \phi_f + \chi_c \phi_c \Leftrightarrow \phi_c = \frac{\phi_{obs} - \chi_f \phi_f}{\chi_c} \quad (S1)$$

NMR experiments were run on a Bruker AMX 400 instrument operating at 400 MHz (^1H) and 101 MHz (^{13}C). The solutions for NMR were prepared in D_2O and the pD adjusted with DCl or NaOD. Photochemical experiments monitored by NMR and conducted at pD values between 3 and 8, deuterated acetate or phosphate buffers were used. Buffers are required due to proton consumption or release during the *trans*-chalcone/flavylium interconversion. Corrections due to isotope effects were applied using the equation $\text{pD} = \text{pH}^* + 0.4$, where pH^* is the reading taken from the pH meter.³ The mass spectra were obtained in a Ultra-High Resolution Qq-Time-Of-Flight (UHR-QqTOF) mass spectrometer (Bruker-Daltonics). The capillary voltage of the electrospray ionization (ESI) was set to 4500 V. The capillary temperature was 200 °C. The sheath gas flow rate (nitrogen) was set to 4L/min.

Crystals suitable for single-crystal X-ray analysis were grown upon slow cooling of a hot concentrated methanolic solution of **1**. Selected crystals were covered with Fomblin (polyfluoroether oil) and mounted on a nylon loop. The data were collected at 296(2) K on a Bruker D8 Venture diffractometer equipped with a Photon 100 CMOS detector, using graphite monochromated Mo-K α radiation ($\lambda = 0.71073 \text{ \AA}$). Data were processed using APEX2 suite software package, which includes integration and scaling (SAINT), absorption corrections (SADABS) and space group determination (XPREP). Structure solution and refinement were done using direct methods with the programs SHELXS-16

inbuilt in APEX and WinGX-Version 2014.1⁴ software packages. All non-hydrogen atoms were refined anisotropically and all the hydrogen atoms were inserted in idealized positions and allowed to refine riding on the parent carbon atom, except for H1 (OH group) that was deduced by inspection of electron density maps. Crystals were of poor quality leading to an overall poor data quality and to a high R_{int} value. The final refinement showed a disordered co-crystallized H₂O molecule and therefore, the SQUEEZE utility in PLATON⁵ was used to remove its contribution to the overall intensity data. The electron density modelled by SQUEEZE is consistent with around 2.8 water molecules per unit cell (ca. 28 electrons for a volume of ca. 102 Å³), corresponding to about 0.7 water molecules per molecule of **1**. The molecular diagrams were drawn with ORTEP-3 for windows and Mercury, included in the software package.^{6,7} Table S1 contains crystallographic experimental data and structure refinement parameters. CCDC 1810850 contains the supplementary crystallographic data for this paper. The data can be obtained free of charge from The Cambridge Crystallographic Data Centre via www.ccdc.cam.ac.uk/structures.

Mathematical Model and Fitting Procedures. The sequential 2:1 host:guest complexation can be described by the two equilibrium reactions shown in Scheme S1.



Scheme S1 – 2:1 sequential binding equilibria.

According to Scheme S1 the following equations can be written:

$$[G]_0 = [G] + [C_{11}] + [C_{21}] \quad (\text{S2})$$

$$[CB7]_0 = [CB7] + [C_{11}] + 2[C_{21}] \quad (S3)$$

$$K_{11} = \frac{[C_{11}]}{[CB7][G]} \quad (S4)$$

$$K_{21} = \frac{[C_{21}]}{[CB7][C_{11}]} \quad (S5)$$

After some algebraic manipulations, the following equations are obtained:

$$[G] + K_{11}[CB7][G] + K_{11}K_{21}[CB7]^2[G] - [G]_0 = 0 \quad (S6)$$

$$[CB7] + K_{11}[CB7][G] + 2K_{11}K_{21}[CB7]^2[G] - [CB7]_0 = 0 \quad (S7)$$

The system of equations was solved numerically using the Newton-Raphson algorithm (in matrix form) implemented in a conventional spreadsheet software to calculate the equilibrium concentrations of CB7 and G.⁸ These values are used along with equations S4 and S5 to calculate the concentration of complexes for a given set of K_{11} and K_{21} values.

Alternatively, equation S6 can be written as:

$$[G] = \frac{[G]_0}{1 + K_{11}[CB7] + K_{11}K_{21}[CB7]^2} \quad (S8)$$

and combined with equation S7 to give the cubic equation S9:⁹

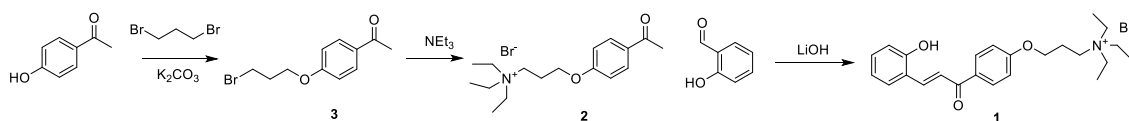
$$\begin{aligned} K_{11}K_{21}[CB7]^3 + (K_{11} + 2K_{11}K_{21}[G]_0 - K_{11}K_{21}[CB7]_0)[CB7]^2 \\ + (K_{11}[G]_0 - K_{11}[CB7]_0 + 1)[CB7] - [CB7]_0 = 0 \end{aligned} \quad (S9)$$

The solution of this cubic equation, that can be also obtained numerically using the Newton-Raphson algorithm, leads to the equilibrium concentration of CB7. Then, the equilibrium concentrations of all other species can be directly obtained from equations S8, S4 and S5.

The observed spectroscopic signal (S_{obs}), such as chemical shifts, absorbance or fluorescence intensity, in the presence of host, is given by equation S10 where S_G is the guest signal observed in the absence of host, and S_{11} and S_{21} are the limiting spectroscopic signals of the 11 and 21 complexes, respectively. The experimental data is fitted to equation S10, using the concentrations numerically determined as described above, and the Solver tool from Excel used to optimize the K_{11} , K_{21} , S_G , S_{11} and S_{21} parameters through a least squares minimization. This spreadsheet template is available from the authors upon request.

$$S_{obs} = \frac{S_G[G] + S_{11}[C_{11}] + S_{21}[C_{21}]}{[G]_0} \quad (S10)$$

Synthesis and Characterization



Scheme S2. Synthetic strategy adopted to synthesize *trans*-chalcone **1**.

1-(4-(3-bromopropoxy)phenyl)ethan-1-one (3). The synthesis of this compound was adapted from a previous report.¹⁰ To a solution of 4-hydroxyacetophenone (6 g, 0.044 mol, 1 eq.) and 1,3 dibromopropane (22.61 mL, 0.223 mol, 5 eq) in acetonitrile (80 mL), K_2CO_3 (40 g, 0.289 mol) and a catalytic amount of KI (0.71g, 4.41 mmol, 0.1 eq) were added. The mixture was stirred for 24 hours at reflux. After cooling to RT, the solid was filtered and the solvent was removed under reduced pressure. A yellow oil was obtained which was diluted with ethyl acetate (15 mL) and washed with water (3x15 mL). The organic phase was dried with $MgSO_4$ and the solvent removed by rotary evaporation. The product was purified by flash chromatography using polarity

gradient from hexane:ethyl acetate 10:1 to 2:1. After evaporation of the solvent a viscous oil was obtained (6.21 g, 55 %). ^1H NMR (400 MHz, Chloroform- d) δ 7.956 (d, $J = 9.4$ Hz, 2H), 6.962 (d, $J = 8.9$ Hz, 2H), 4.202 (t, $J = 5.8$ Hz, 2H), 3.633 (t, $J = 6.4$ Hz, 2H), 2.582 (s, 3H), 2.370 (p, $J = 6.1$ Hz, 2H).

3-(4-acetylphenoxy)- N,N,N -triethylpropan-1-ammonium bromide (2). 1.35 mL of triethylamine (9.7mmol, 10eq) was added dropwise to 5 mL solution of **3** (250mg, 0.97mmol) dissolved in acetone. The reaction mixture was refluxed for 24 hours. After cooling to RT, addition of diethyl ether induced the separation of a viscous brown oil. The oil was dissolved in the minimum quantity of methanol and re-separated by addition of diethyl ether. The resulting viscous material was dried in high-vacuum to give 207mg of **2** in 76% yield. ^1H NMR (400 MHz, Acetone- d_6) δ / ppm 7.98 (d, $J = 9.0$ Hz, 2H), 7.10 (d, $J = 9.0$ Hz, 2H), 4.36 (t, $J = 5.8$ Hz, 2H), 3.82 – 3.71 (m, 2H), 3.65 (q, $J = 7.3$ Hz, 6H), 2.53 (s, 3H), 2.46 – 2.36 (m, 2H), 1.45 (t, $J = 7.3$ Hz, 9H). ^{13}C NMR (101 MHz, Acetone- d_6) δ / ppm 195.70, 162.46, 130.70, 130.42, 114.18, 64.77, 54.20, 53.06, 25.66, 22.10, 7.26. HRMS (ESI) m/z calcd for $\text{C}_{17}\text{H}_{28}\text{NO}_2^+$ [M^+]: 278.2115; found: 278.2118.

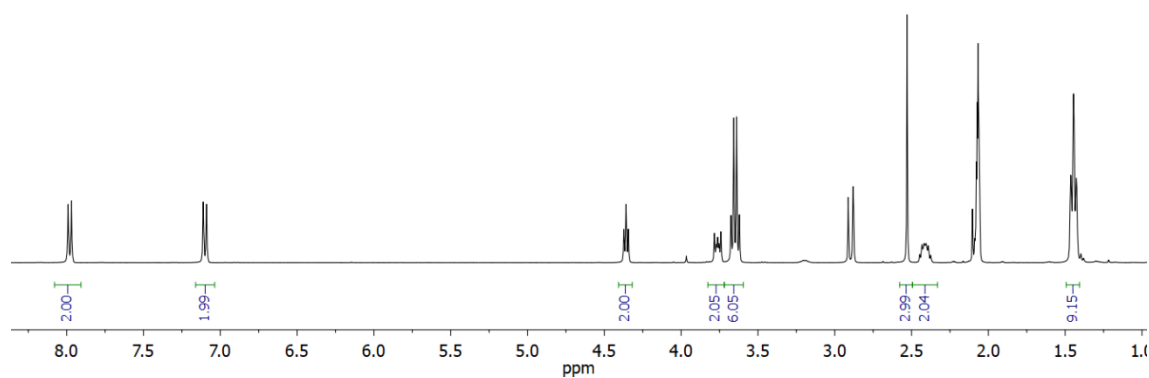


Figure S1. ^1H NMR spectrum of acetophenone **2** in acetone- d_6 .

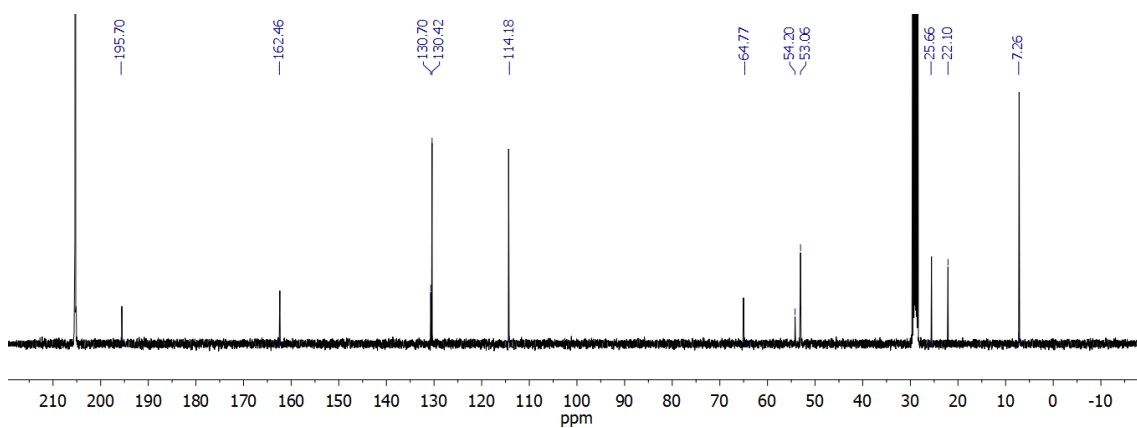


Figure S2. ^{13}C NMR spectrum of acetophenone **2** in acetone- d_6 .

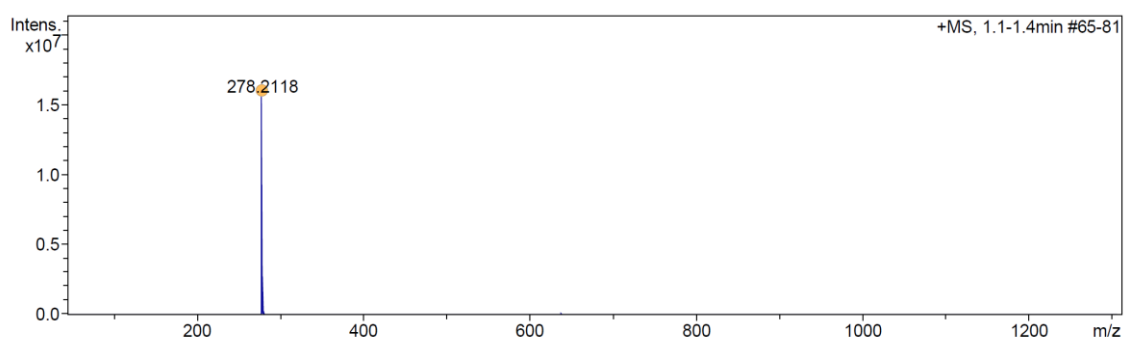


Figure S3. ESI-MS spectrum of acetophenone **2**.

***trans*-Chalcone 1.** Acetophenone **2** (121mg, 0.435mmol) and salicylaldehyde (0.068 mL, 0.65mmol, 1.5 equiv.) were dissolved in 1.5 mL of methanol. The reaction mixture was cooled in an ice bath and 72.7 mg of LiOH.H₂O (1.73mmol, 4equiv.) was carefully added. After 24 hours at 50 °C, the orange solution was neutralized with a methanolic solution of HBr 1M. After evaporation of the solvents, the brown residue was washed several times with diethyl ether and recrystallized from methanol to afford pale yellow crystals of **1** (73 mg, 36% yield). The obtained crystals were suitable for X-Ray diffraction. ^1H NMR (400 MHz, Methanol- d_4) δ / ppm 8.12 (d, $J = 15.4$ Hz, 1H), 8.09 (d, $J = 8.2$ Hz 2H), 7.84 (d, $J = 15.7$ Hz, 1H), 7.69 (d, $J = 7.7$ Hz, 1H), 7.27 (t, $J = 7.8$ Hz, 1H), 7.12 (d, $J = 8.6$ Hz, 2H), 6.95 – 6.87 (m, 2H), 4.25 (t, $J = 5.6$ Hz, 2H), 3.57 – 3.37 (m, 8H), 2.33 – 2.19 (m, 2H), 1.37 (t, $J = 7.3$ Hz, 9H). ^{13}C NMR (101 MHz,

Methanol-*d*₄) δ / ppm 190.10, 162.36, 157.46, 140.53, 131.57, 131.49, 130.62, 128.97, 121.80, 120.93, 119.45, 115.72, 114.11, 64.45, 53.88, 52.58, 21.56, 6.26. HRMS (ESI) *m/z* calcd for C₂₄H₃₂NO₃⁺ [M⁺]: 382.2377; found: 382.2389.

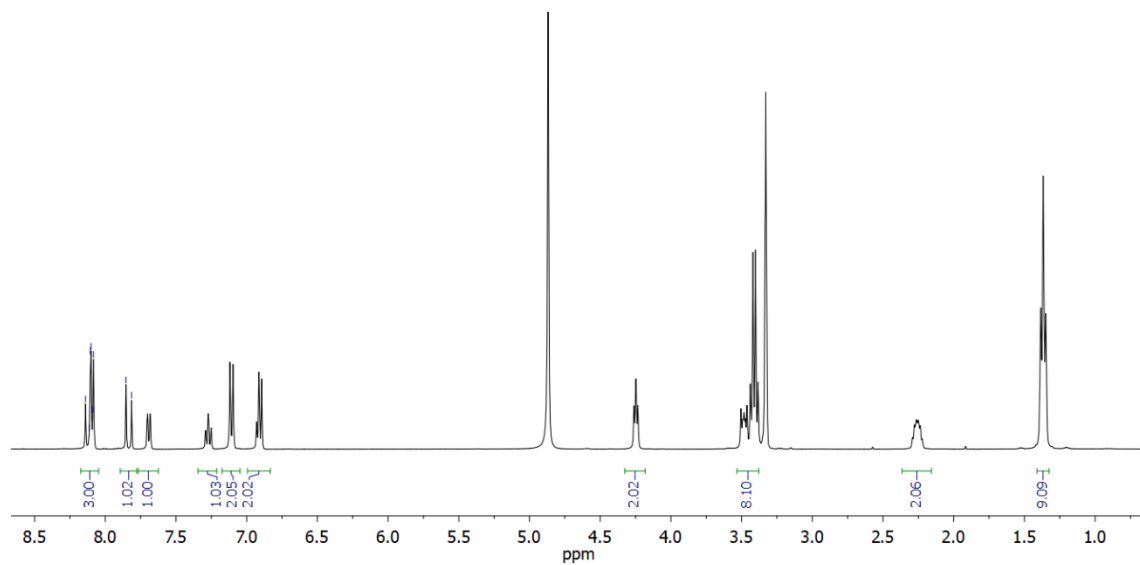


Figure S4. ¹H NMR spectrum of trans-chalcone **1** in CD₃OD.

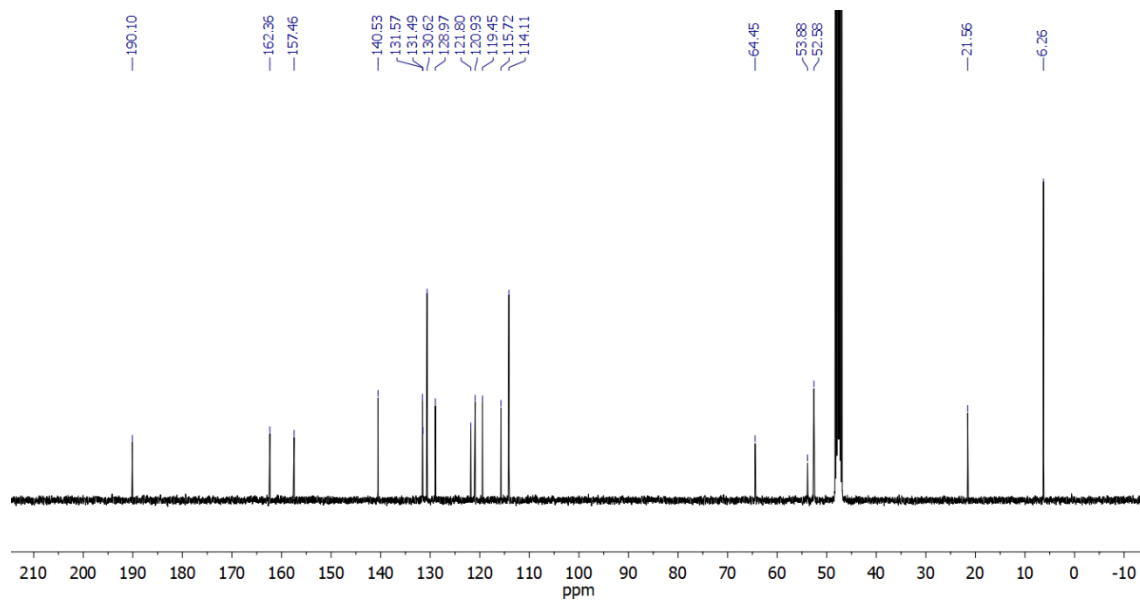


Figure S5. ¹³C NMR spectrum of trans-chalcone **1** in CD₃OD.

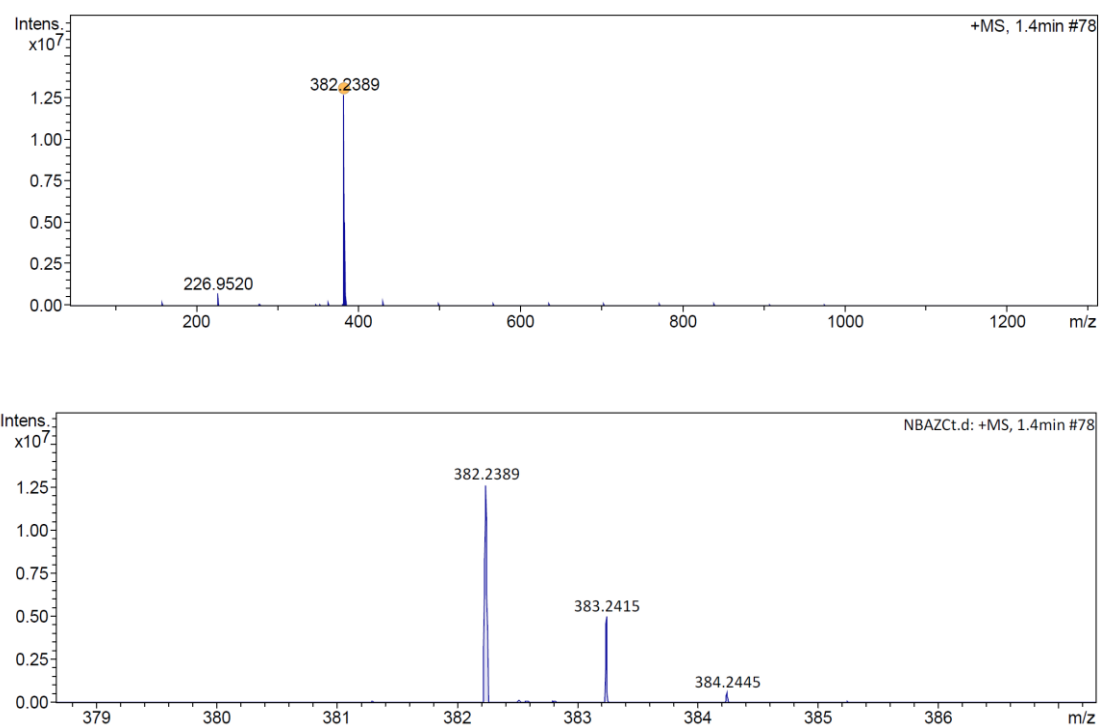


Figure S6. ESI-MS spectrum of trans-chalcone **1**.

Table S1. Crystal data and structure refinement for the title compound.

Empirical formula	$C_{24}H_{32}BrNO_3 \cdot 0.7(H_2O)$	
Formula weight	462.41	
Temperature	296(2) K	
Wavelength	0.71073 Å	
Crystal system	Monoclinic	
Space group	P 21/c	
Unit cell dimensions	$a = 18.980(3)$ Å	$\alpha = 90^\circ$.
	$b = 10.7749(16)$ Å	$\beta = 93.315(9)^\circ$.
	$c = 11.4258(18)$ Å	$\gamma = 90^\circ$.
Volume	$2332.8(6)$ Å ³	
Z	4	
Density (calculated)	1.317 Mg/m ³	

Absorption coefficient	1.786 mm ⁻¹
F(000)	968
Crystal size	0.300 x 0.100 x 0.030 mm ³
Theta range for data collection	2.174 to 25.083°.
Index ranges	-22<=h<=22, -12<=k<=12, -13<=l<=13
Reflections collected	41450
Independent reflections	4118 [R(int) = 0.2595]
Completeness to theta = 25.083°	99.3 %
Refinement method	Full-matrix least-squares on F ²
Data / restraints / parameters	4118 / 0 / 266
Goodness-of-fit on F ²	0.963
Final R indices [I>2sigma(I)]	R1 = 0.0545, wR2 = 0.1105
R indices (all data)	R1 = 0.1422, wR2 = 0.1288
Largest diff. peak and hole	0.470 and -0.410 e.Å ⁻³

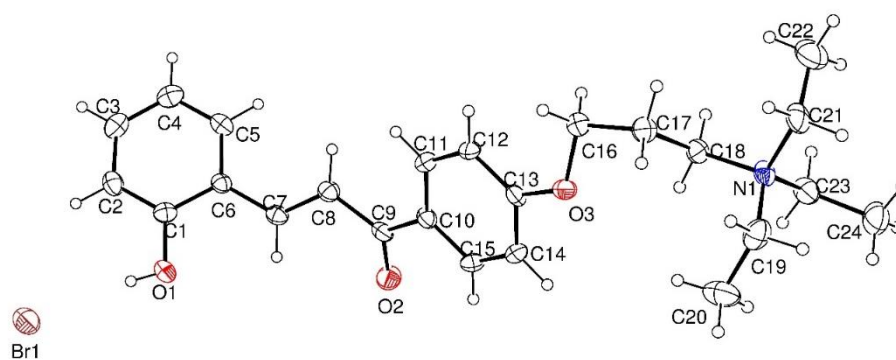


Figure S7. ORTEP-3 diagram of the title compound, using 30% probability level ellipsoids..

Additional spectroscopic data

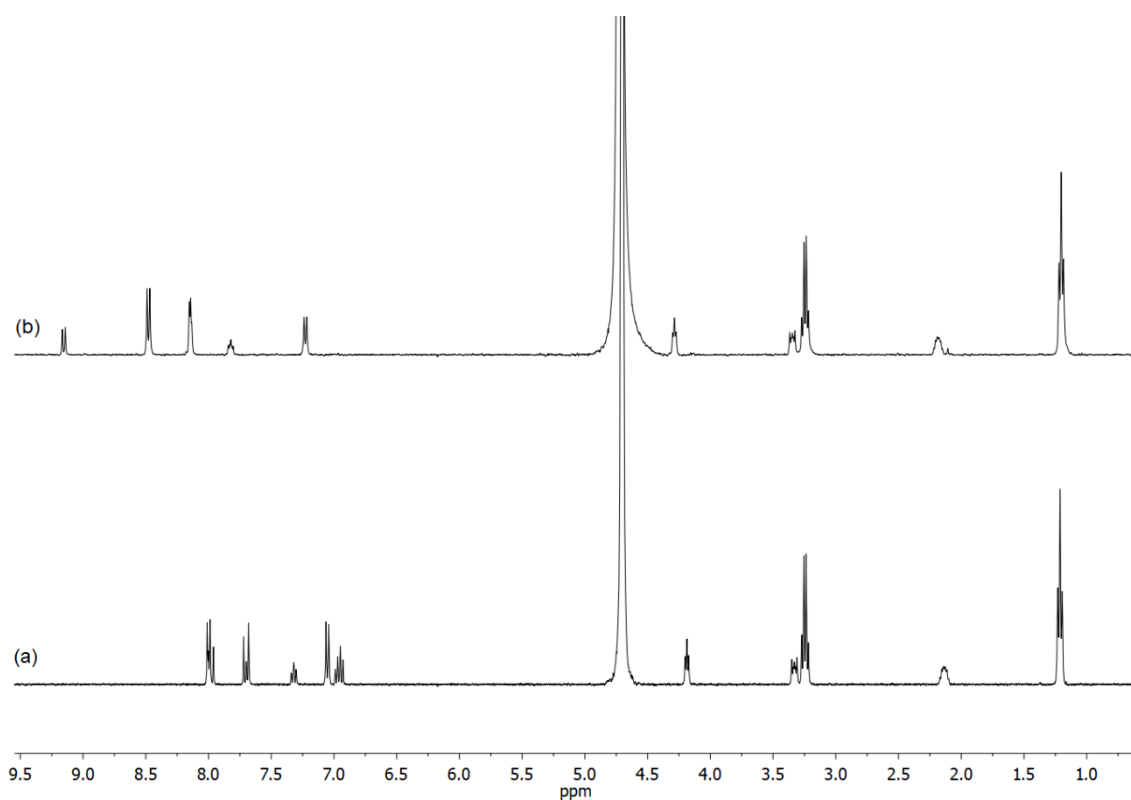


Figure S8. ¹H NMR spectra of (a) *trans*-chalcone **1** in D₂O (0.4 mM) at neutral pD and (b) flavylum cation **2** obtained after 365 nm light irradiation of **1** (0.4 mM) directly in the NMR tube at in 0.1 M DCl. The residual HDO chemical shift was not corrected for the pD-dependence.

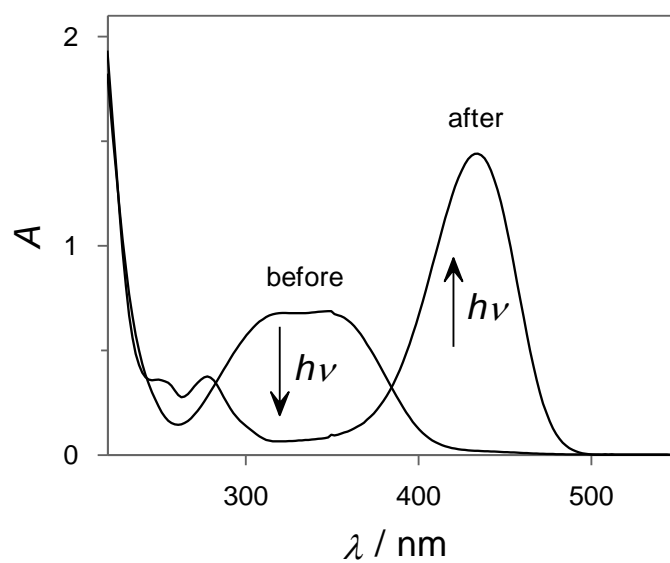


Figure S9. UV-Vis absorption spectra of *trans*-chalcone **1** (33 μM) in citric acid buffer (10 mM) aqueous solution at pH = 2.2 before and after 30 minutes of irradiation with a 365 nm light source. The

disappearance of the characteristic absorption band of **1** and the appearance of a new band centered 434 nm is compatible with quantitative photoinduced formation of **2**.

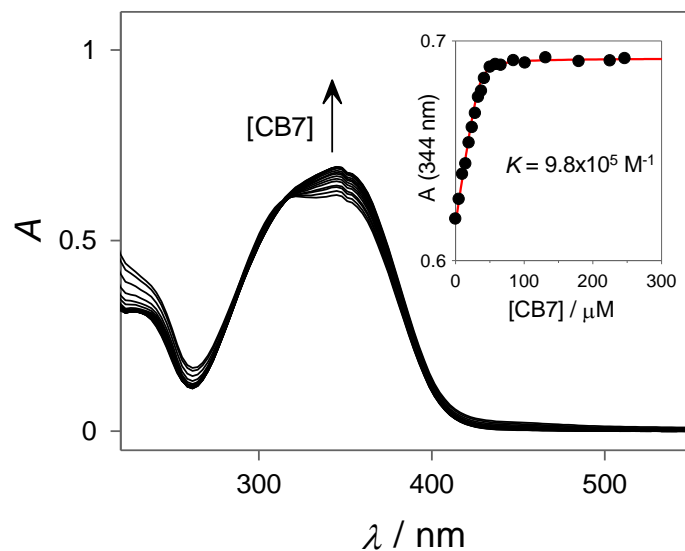


Figure S10. UV-Vis spectral modifications observed after adding increasing amounts of CB7 to a solution of *trans*-chalcone **1** (35 μM) at pH = 6.5. The inset shows the absorbance at 334 nm represented against the concentration of CB7 and the corresponding fit (red line) to a 1:1 binding model.

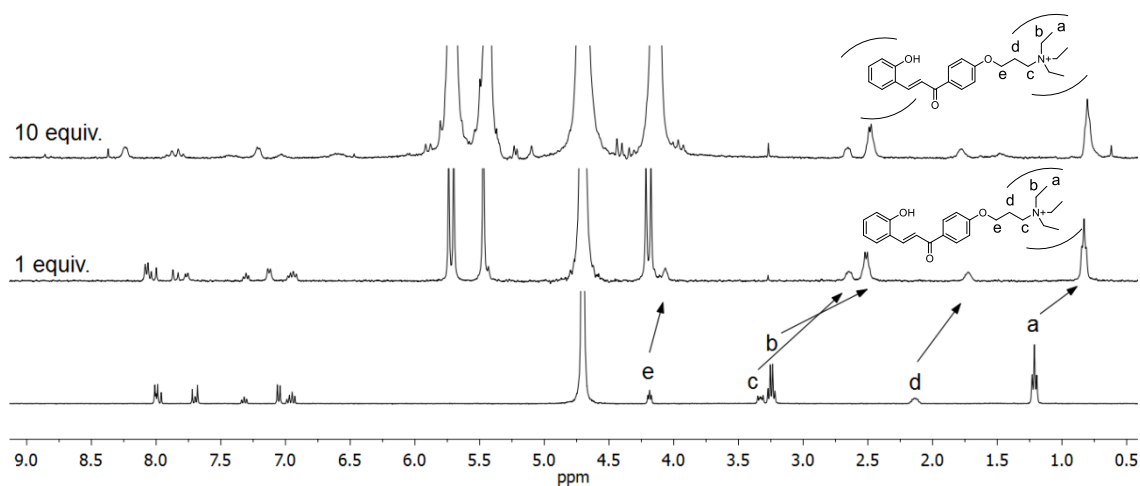


Figure S11. ¹H NMR spectra of *trans*-chalcone **1** in D₂O (0.4 mM) at neutral pH in the absence and in the presence of 1 and 10 equivalents of CB7.

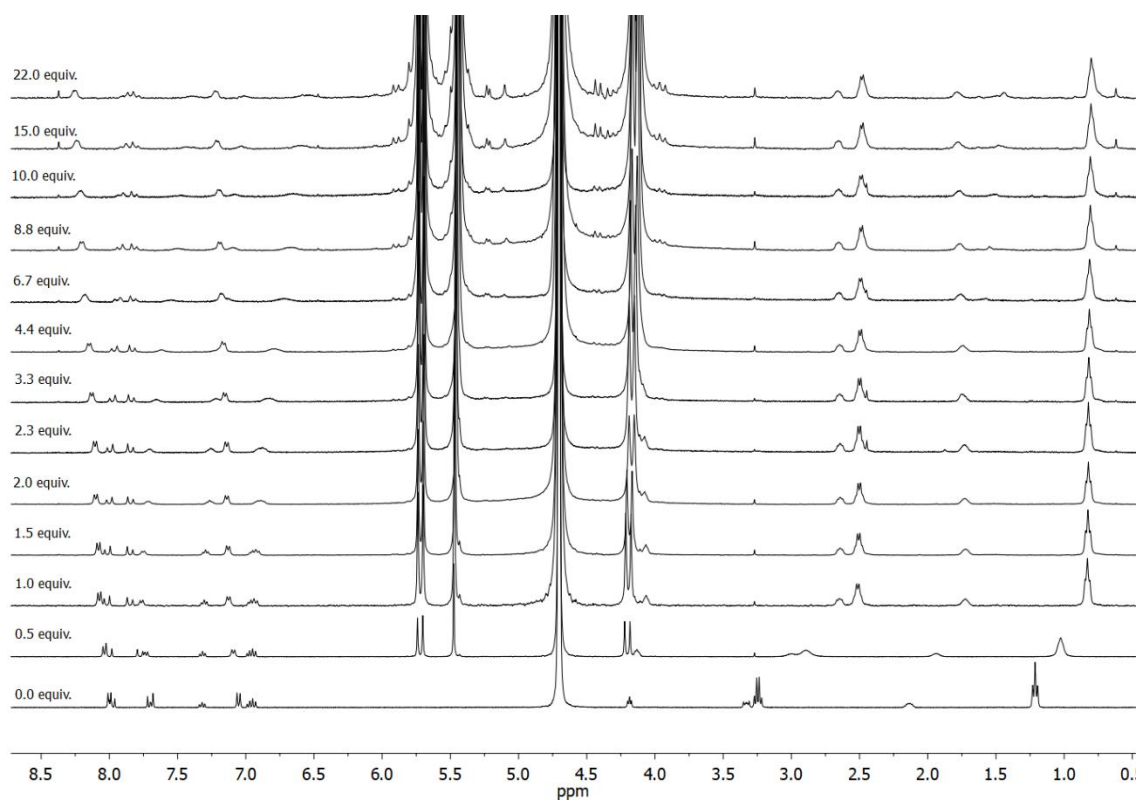


Figure S12. ^1H NMR spectra of *trans*-chalcone **1** in D_2O (0.4 mM) at neutral pD in the absence and in the presence of increasing concentrations of CB7.

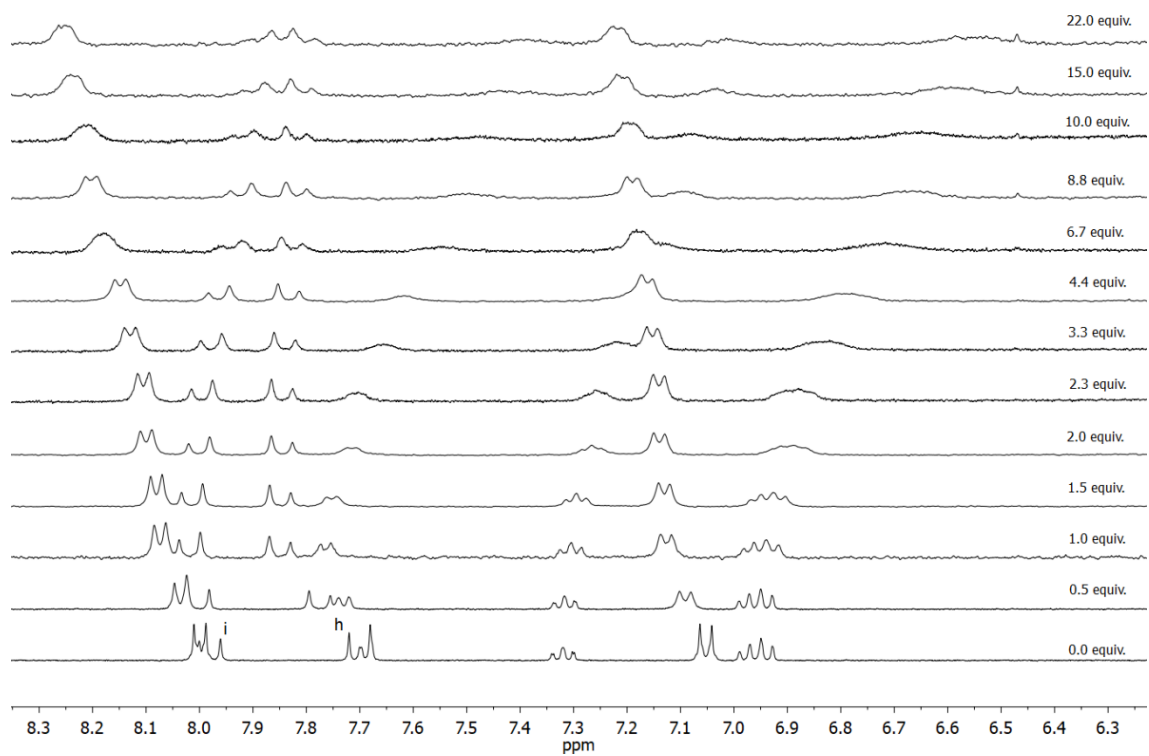


Figure S13. Expansion of the aromatic region of the ^1H NMR spectra show in Figure S12. Protons *h* and *i* (see manuscript for proton labeling) were used for the determination of the K_{21} binding constant (see below).

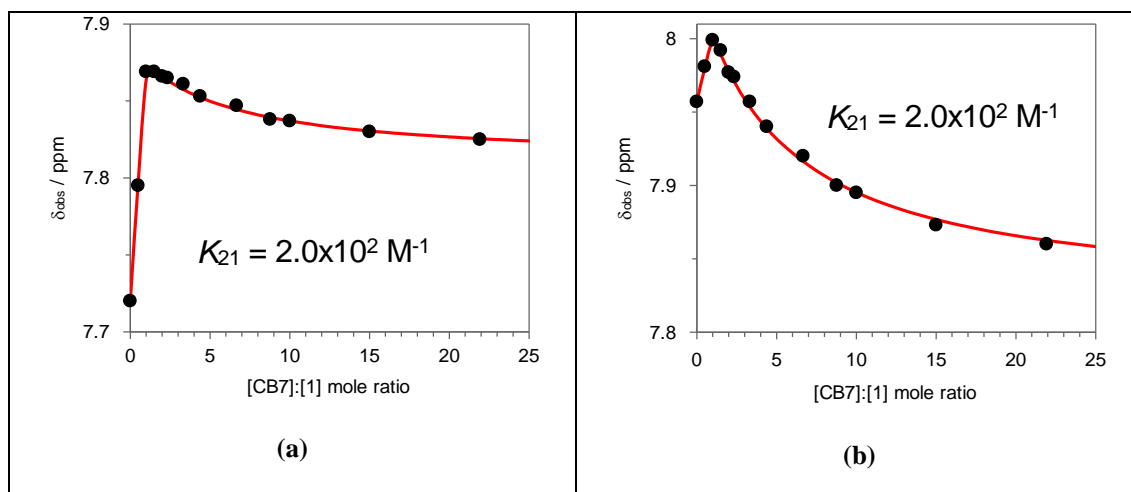


Figure S14. Observed NMR chemical shifts (δ_{obs}) for protons (a) *h* and (b) *i* represented against the $[\text{CB7}]:[1]$ mole ratio. The data was globally fitted (red line) to a 2:1 host:guest binding model with K_{11} fixed at $9.8 \times 10^5 \text{ M}^{-1}$ (the NMR concentration is too high to measure this K with accuracy).

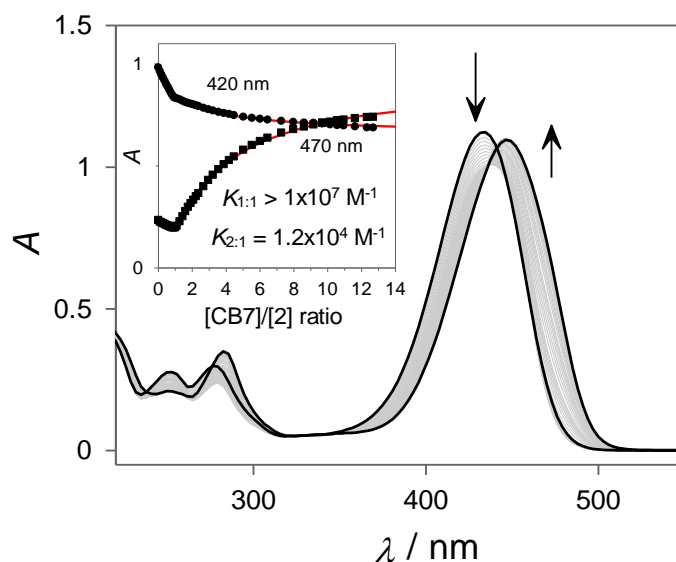


Figure S15. UV-Vis spectral modifications observed after adding increasing amounts of CB7 to a solution of flavylum 2 (26 μM) at pH = 2 (HCl = 0.01 M). The inset shows the absorbance at 420 nm (circles) and at 470 nm (squares) represented against the concentration of CB7 and the corresponding fit (red line) to a sequential 2:1 binding model.

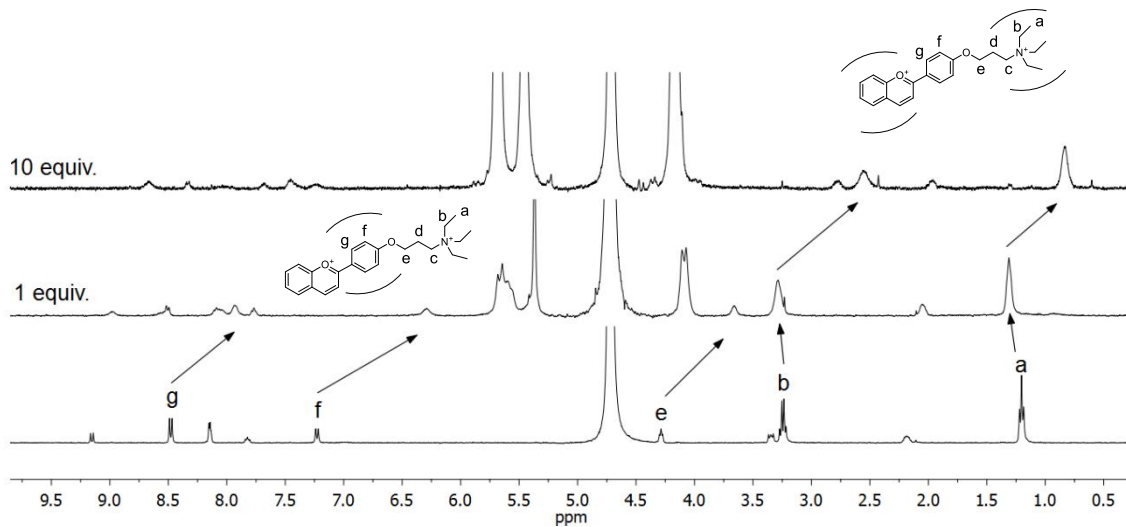


Figure S16. ^1H NMR spectra of flavilyium **2** in D_2O (0.4 mM) at $\text{pD} = 1$ in the absence and in the presence of 1 and 10 equivalents of CB7.

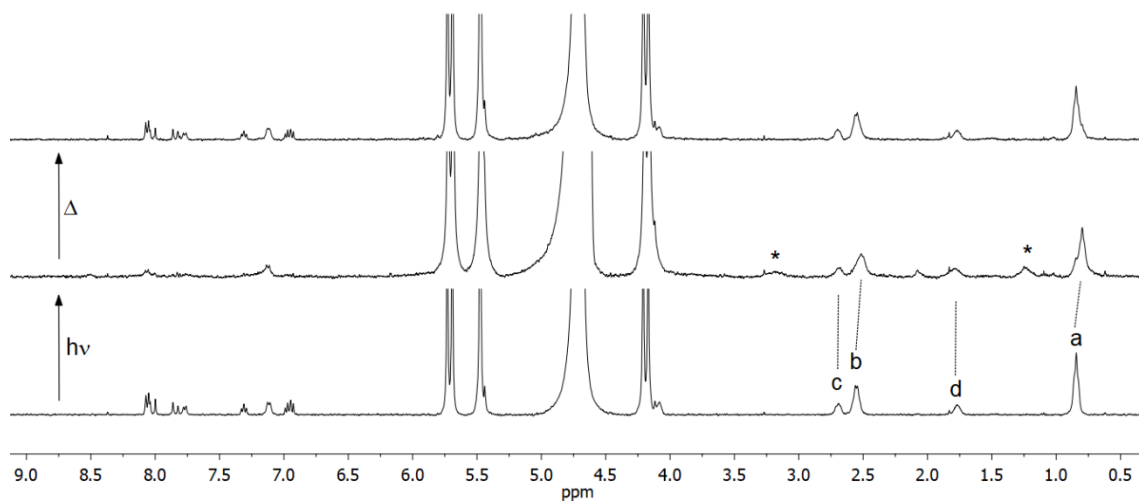


Figure S17. ^1H NMR spectra of **1:CB7** in D_2O (0.4 mM) at $\text{pD} = 7.4$ (phosphate buffer 5 mM) in the presence of 1 equivalent of CB7. Before (bottom), after irradiation (middle) and upon standing in dark for 2 hours at $80\text{ }^\circ\text{C}$. The signals marked with * are assigned to the residual formation of **2:CB7** at this pD value.

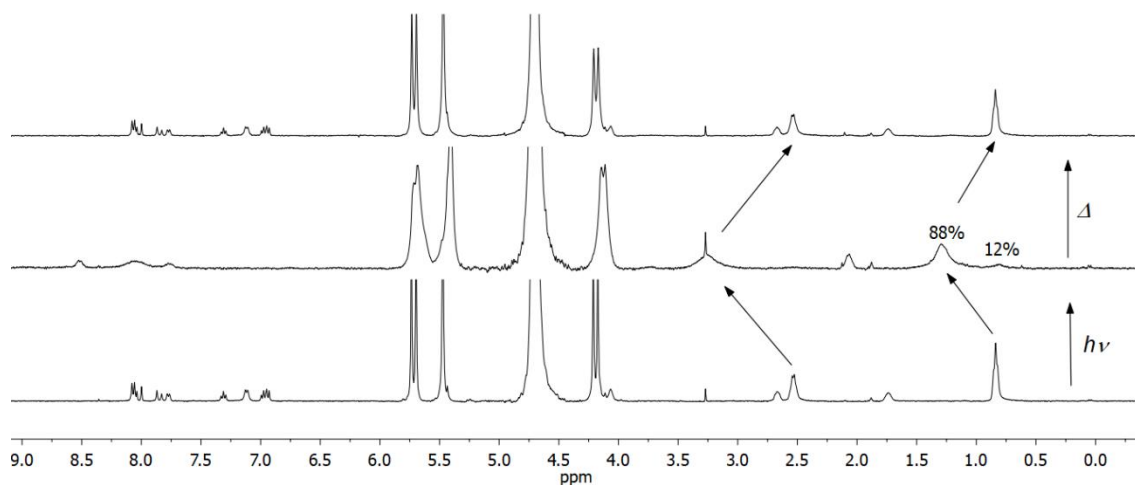


Figure S18. ^1H NMR spectra of **1:CB7** in D_2O (0.4 mM) at $\text{pD} = 5.3$ (acetate buffer 10 mM) in the presence of 1 equivalent of CB7. Before (bottom), after irradiation (middle) and upon standing in dark for overnight at 60°C . Signal broadening is observed probably due to slow/intermediate equilibrium between the complexed flavylum species (88%) and complexed *cis*-chalcone/hemiketal (12%); see Scheme 3 in the manuscript.

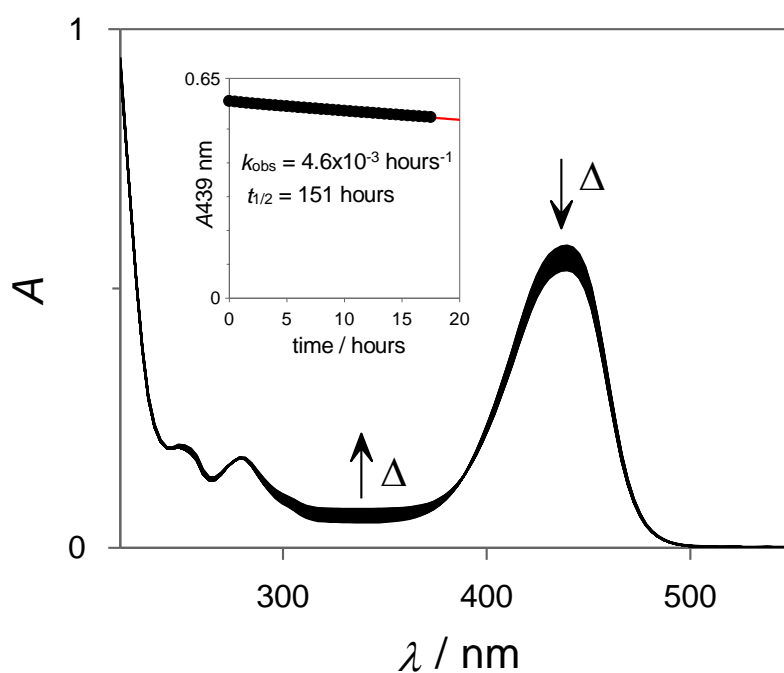


Figure S19. UV-Vis spectral modifications observed for the thermal recovery (25°C) of a fresh solution of pseudorotaxane **2:CB7** (equimolar concentrations of both components $15\ \mu\text{M}$), generated by irradiation of **1:CB7** at $\text{pH} = 5$ (citrate buffer 10 mM). The observed rate constant was estimated from the

slope of the Absorbance vs time data (see inset) using the initial rate method: $k_{\text{obs}} = \text{slope}/A_0$ where A_0 the Absorbance at time = 0. The half-life is given by $t_{1/2} = \ln(2)/k_{\text{obs}}$.

References

- 1 N. Basílio, V. Petrov and F. Pina, *ChemPlusChem*, 2015, **80**, 1779–1785.
- 2 B. Soep, A. Kellmann, M. Martin and L. Lindqvist, *Chem. Phys. Lett.*, 1972, **13**, 241–244.
- 3 P. K. Glasoe and F. A. Long, *J. Phys. Chem.*, 1960, **64**, 188–190.
- 4 L. J. Farrugia, *J. Appl. Crystallogr.*, 2012, **45**, 849–854.
- 5 A. L. Spek, *Acta Cryst.*, 2015, **C71**, 9–18.
- 6 L. J. Farrugia, *J. Appl. Crystallogr.*, 1997, **30**, 565–565.
- 7 C. F. Macrae, P. R. Edgington, P. McCabe, E. Pidcock, G. P. Shields, R. Taylor, M. Towler and J. van de Streek, *J. Appl. Crystallogr.*, 2006, **39**, 453–457.
- 8 S. del Piero, A. Melchior, P. Polese, R. Portanova and M. Tolazzi, *Ann. Chim.*, 2006, **96**, 29–49.
- 9 P. Thordarson, *Chem. Soc. Rev.*, 2010, **6**.
- 10 M. Al-Smadi, N. Hanold, H. Kalbitz and H. Meier, *Synthesis*, 2009, 2539–2546.